ACS Catalysis

pubs.acs.org/acscatalysis Letter

Low-Temperature Ammonia Production during NO Reduction by CO Is Due to Atomically Dispersed Rhodium Active Sites

Chithra Asokan, Yang Yang, Alan Dang, Andrew "Bean" Getsoian, and Phillip Christopher*

Cite This: *ACS Catal.* 2020, 10, 5217−5222 Read Online

ACCESS | Metrics & More | Article Recommendations | Supporting Information

ABSTRACT: Rhodium plays a key role in three-way catalysts to control NO_x emissions in gasoline engines primarily through the reduction of NO by CO. Despite extensive investigation, there remains uncertainty about NO reduction mechanisms. Particularly, it is unknown which sites are responsible for the unselective reduction of NO to NH_3 under light-off conditions or in CO-rich feed. By varying Rh catalyst structure from atomically dispersed species to clusters on Al_2O_3 and CeO_2, we provide evidence that in the reduction of NO by CO with co-fed H_2O, low-temperature NH_3 formation occurs on atomically dispersed Rh sites, whereas high-nuclearity Rh clusters are selective to N_2.

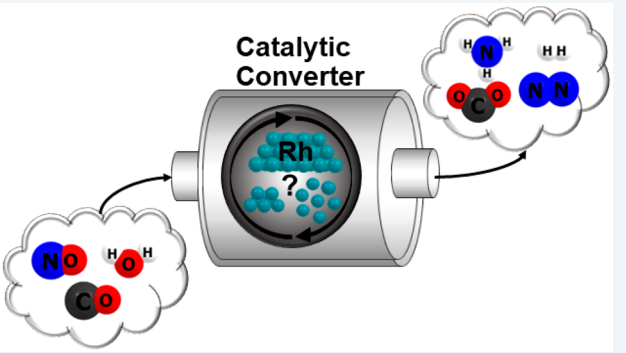

KEYWORDS: *atomically dispersed Rh, NO reduction, three-way catalysts (TWC), single-atom catalysts, ammonia*

In gasoline-powered vehicles, a three-way catalyst (TWC) is used to control the emission of criteria pollutants (NO_x, CO, and hydrocarbons). While oxidation of CO and hydrocarbons results in CO_2 and H_2O emissions, simultaneous reduction of NO_x can produce not only N_2 (the desired product) but also NH_3 and N_2O. These products are environmentally detrimental: N_2O is a potent greenhouse gas, and atmospheric NH_3 is linked to particulate formation, ecosystem eutrophication, and decreased resilience of vegetation to exasperation, including parasites and drought.[1−4] To guide the formulation and operation of TWCs to minimize NH_3 and N_2O formation while maintaining maximal control over NO_x emissions, greater understanding of the mechanisms of NO_x reduction in TWCs is required.

Although it is generally observed that richer air/fuel ratios lead to increasing NH_3 selectivity during NO_x reduction, selectivity is also sensitive to catalyst formulation.[5−8] Rh is generally considered to be both more active for NO_x reduction and more selective to N_2 than Pd.[9] However, Rh-only catalysts can also generate NH_3 under light-off conditions or in feeds containing excess reductant or a source of hydrogen.[10] While pathways leading to NH_3 formation on Pd have been investigated in detail, NH_3 formation on Rh has received little attention.[11] Many fundamental studies of NO reduction on Rh model catalysts have been conducted under conditions that avoid NH_3 formation because it adds challenges to elucidating N_2 production pathways.[12−14] Even under simplified conditions (e.g., reduction of NO by CO), mechanistic understanding on single crystals is inconsistent with results obtained on supported particles (and different investigators obtain different results on the latter), underscoring the need for a new look at structure−function relationships for Rh catalysts.[13−18]

Developing structure−function relationships for heterogeneous Rh catalysts is complicated because Rh is known to speciate between atomically dispersed species and metal clusters, depending on environmental conditions, particularly under environments containing CO, NO, H_2, and H_2O, which are abundant in exhaust streams.[19,20] This is important because TWCs Rh weight loadings are commonly lower than ∼0.3%, where a mix of Rh nanoparticles, small clusters, and atomically dispersed species coexist.[21] While the reduction of NO by CO is well studied for Rh nanoparticles and extended Rh surfaces, the role of atomically dispersed species in this chemistry, particularly under relevant conditions with H_2O in the feed, has not been addressed.[16,22−28] This is a potential key to understanding mechanistic pathways in TWCs because atomically dispersed Rh species on oxide supports are known to exhibit distinct selectivity in catalytic processes compared with Rh clusters.[29−32]

Here, we elucidate structure−function relationships for oxide supported Rh catalysts for the reduction of NO by CO under dry conditions and in the presence of H_2O. Under dry conditions atomically dispersed Rh species are less reactive

Received: March 17, 2020
Revised: April 15, 2020
Published: April 15, 2020

https://dx.doi.org/10.1021/acscatal.0c01249
ACS Catal. 2020, 10, 5217−5222

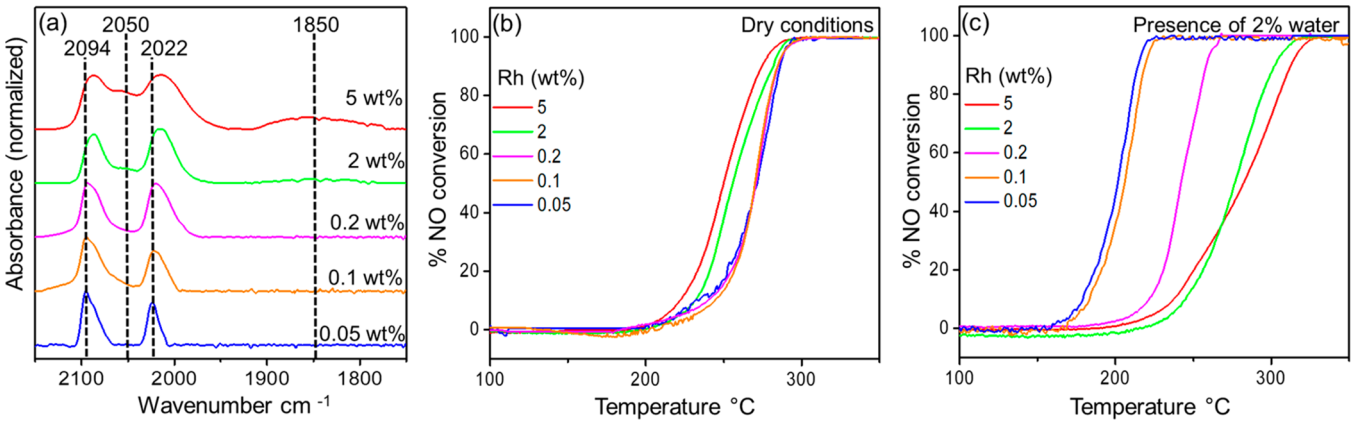

Figure 1. (a) CO probe molecule FTIR spectra collected for Rh/γ- Al_2O_3 with varying Rh wt % after in situ 350 °C oxidation for 30 min and 100 °C reduction in H_2 for 60 min, followed by saturation with 10% CO at 20 °C. The spectra were normalized by the highest intensity feature in this region and vertically separated for clarity. (b) NO conversion (%) as a function of temperature for a linear temperature ramp of 5 °C/min in dry conditions (5000 ppm of CO/1000 ppm of NO, and (c) wet conditions (5 °C/min in 2% H_2O/5000 ppm of CO/1000 ppm of NO) for the series of catalysts characterized in (a).

than Rh clusters. The addition of H_2O to the feed significantly promotes the reactivity of atomically dispersed Rh and results in 100% selectivity to NH_3 at temperatures <200 °C on both Al_2O_3 and CeO_2 supports. Rh clusters are less reactive than atomically dispersed species when H_2O is co-fed and the reaction primarily leads to N_2 formation. This revelation provides a basis for examining impacts of catalyst formulation for minimizing NH_3 production.

To facilitate the development of structure−function relationships, catalysts were synthesized using $Rh(NO_3)_3$ at varied weight loadings on γ-Al_2O_3 (Sasol, Puralox TH100/150, 150 m^2/g), Figure S1.[33] The Rh weight loading was varied from 0.05 to 5 wt % to control the distribution of Rh species from atomically dispersed to clusters and nanoparticles. Catalysts were ex situ oxidized at 350 °C for 4 h and in situ oxidized at 350 °C for 30 min in O_2, purged with inert, and in situ reduced at 100 °C for 1 h in H_2 prior to characterization or reactivity measurements.

Characterization of Rh structures present on the catalysts was accomplished by using CO probe molecule FTIR spectroscopy.[24,27,29,34−39] This approach is particularly useful for characterizing supported atomically dispersed Rh species because of unique vibrational signatures of adsorbed CO as compared with Rh clusters. In 1957, Garland and Yang first hypothesized that CO adsorption on atomically dispersed Rh resulted in the formation gem-dicarbonyl ($Rh(CO)_2$) species with characteristic symmetric and asymmetric CO stretches at ∼2090 and 2020 cm^{-1}, respectively.[40] On Rh nanoparticle and cluster surfaces, CO adsorbs in linear and bridge bound geometries that have characteristic stretches at ∼2070−2050 and ∼1950−1850 cm^{-1}, respectively.[40−44] These Rh structural assignments based on CO FTIR have been substantiated by nuclear magnetic resonance (NMR) measurements, X-ray photoelectron spectroscopy (XPS), X-ray absorption spectroscopy (XAS), and high-angle annular dark-field scanning transmission electron microscopy (HAADF-STEM) imaging.[35,45−48] For example, structure−function relationships for Rh/TiO_2 based catalysts for the reduction of CO_2 developed via characterization based on CO FTIR and reactivity measurements were further supported later based on STEM and XPS analysis.[29,35,48] Thus, while applying a full suite of characterization tools is necessary when studying systems containing new catalyst compositions and structures, CO FTIR is a well-established approach for developing structure−function relationships for supported Rh-based catalysts.[29,35,49,50]

Figure 1a shows CO probe molecule IR spectra for 0.05, 0.1, 0.2, 2, and 5 wt % Rh/Al_2O_3. At low Rh wt % (0.05, 0.1, and 0.2%), the IR spectra were dominated by CO stretches at 2094 and 2022 cm^{-1} associated with the atomically dispersed $Rh(CO)_2$ species. The CO stretching bands associated with the $Rh(CO)_2$ species show asymmetry, suggesting the existence of multiple coordination environments to the support (for example, based on the proximity to hydroxyl species with varying characteristics).[39−41,51,52] Temperature-programmed desorption (TPD) measurements of CO from the 0.1 wt % Rh sample shows evidence of two distinct $Rh(CO)_2$ species, where CO desorbs at different temperatures, Figure S2. Thus, while the lowest Rh loading samples contain predominantly atomically dispersed species, these species likely reside in various coordination environments on the support. Future work will aim to understand the influence of atomically dispersed Rh coordination environment on reactivity. Evidence for linearly bound CO to small Rh clusters could also be seen on the 0.1 and 0.2 wt % samples based on an increase in absorbance between the $Rh(CO)_2$ stretches. The prevalence of Rh clusters increased with increasing Rh loadings, as evidenced by the stronger absorbance associated with CO stretches at 2070 and 1850 cm^{-1} associated with linear and bridge-bound CO. The fraction of exposed Rh sites existing as atomically dispersed species was estimated by integrating the peak areas associated with CO on various adsorption sites and accounting for adsorption stoichiometry and extinction coefficients, where $Rh(CO)_2$ species have a ∼3-fold larger extinction coefficient than linearly bound CO on Rh clusters.[29,41,43,53] On the basis of this approach, it was estimated that on the 5 wt % Rh sample only ∼ 8% of the exposed Rh sites were atomically dispersed species, while 92% of adsorption sites were at the surface of Rh nanoparticles, see Table S1. Therefore, this series of catalysts presents a decreasing fraction of exposed atomically dispersed Rh species with increasing weight loading.

To develop structure−function relationships over the various Rh catalysts relevant for the start-up regime of TWC operation, "light off" experiments were performed where the

https://dx.doi.org/10.1021/acscatal.0c01249
ACS Catal. 2020, 10, 5217−5222

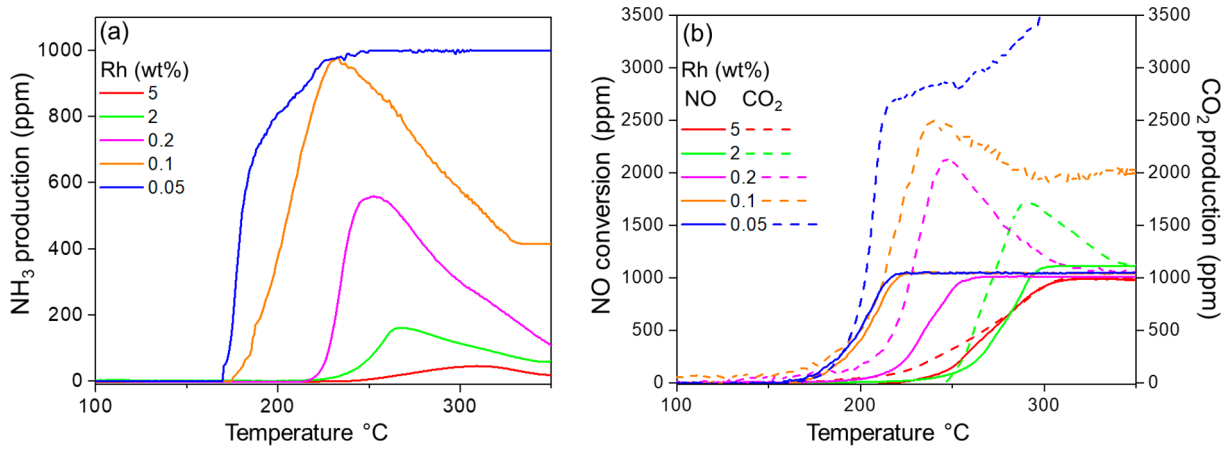

Figure 2. (a) NH_3 production (ppm), (b) NO consumption (solid lines), and CO_2 production (dotted lines) during temperature-programmed reaction at a temperature ramp rate of 5 °C/min in 5000 ppm of CO/1000 ppm of NO/2% of H_2O for the series of catalysts characterized in Figure 1a.

reactor was heated at a controlled linear rate from ambient temperature. CO was chosen as reductant for NO because light offs for CO and NO are known to be coupled on Rh catalysts.[54] In some tests, water was co-fed in order to assess the impact of this important exhaust component on NO_x reduction selectivity. While more complex feeds could also be considered, the CO+NO+H_2O blend was sufficient to achieve the aims of the present study. Catalysts were diluted with purified silicon dioxide (Sigma-Aldrich 84878) to provide a constant loading of 0.2 mg of Rh in the 1 g of total material loaded into the reactor, Table S2. After pretreatment, catalysts were heated at 5 °C/min in a flow of 5000 ppm of CO and 1000 ppm of NO diluted in Ar both in dry and wet conditions (with ∼2% water) at a total flow rate of 200 standard cubic centimeters per minute (sccm).

In dry reaction conditions, all catalysts started converting NO into N_2 at ∼210 °C, but samples with a higher fraction of Rh clusters, 2 and 5 wt % Rh, exhibited increased conversion at lower temperature as compared to samples that contained predominantly atomically dispersed Rh, 0.05, 0.1, and 0.2 wt % Rh, Figure 1b. All catalysts produced 1:1 stoichiometric amounts of CO_2 and N_2 with high selectivity, although a small amount of N_2O was observed at low temperatures, which was independent of Rh loading, see Figure S3. Differences in the light-off curve shapes suggests different rate laws for NO reduction over Rh clusters compared with atomically dispersed Rh species.[55] However, future steady-state measurements are necessary to unravel the underlying kinetics. It is clear that Rh clusters on Al_2O_3 are more effective at catalyzing the reduction of NO by CO under dry conditions, although only by a small amount.

Light-off curves acquired in the presence of H_2O exhibited distinct differences as a function of Rh weight loading, see Figure 1c. The addition of H_2O to the feed promoted the reactivity of lower wt % Rh catalysts, for example, decreasing the onset of measurable NO conversion by ∼50 °C for the 0.05 and 0.1 wt % Rh catalysts. While the 0.2 wt % Rh catalyst exhibited higher light-off temperatures as compared with the 0.05 and 0.1 wt % catalysts, the shape of the light-off curve was similar, suggesting similar kinetic behavior with a fewer number of active sites. For the higher Rh wt % catalysts (2 and 5%), the addition of H_2O to the feed inhibited the onset of NO conversion by ∼10 °C. Thus, while the behavior of all catalysts was similar under dry conditions, stark differences were observed upon the introduction of H_2O to the feed.

Most interestingly, the concentration of NH_3 produced during the wet light-off experiments increased with decreasing Rh wt % and thus with an increase in the relative fraction of atomically dispersed Rh species, Figure 2a. The lowest tested Rh weight loading, 0.05%, exhibited ∼100% NH_3 selectivity with complete NO conversion by ∼210 °C. The 0.1 wt % Rh catalyst converted NO to NH_3 with close to 100% selectivity during the light off, but once 100% NO conversion was reached, NH_3 selectivity declined and N_2 production increased. As the Rh wt % in the catalyst was increased, the selectivity toward N_2 increased and NH_3 production decreased. The amounts of N_2 and N_2O produced during the light off are shown in Figure S4.

We compared NO conversion and CO_2 production to elucidate the stoichiometry of the reactions taking place, see Figure 2b. For the 0.05 and 0.1 Rh wt % catalysts, at the temperature where 100% conversion of NO to NH_3 was reached, 2.5 times more CO_2 was produced than NO consumed. For the 5 Rh wt % catalyst, less than 50 ppm of NH_3 was produced and at the temperature where NO conversion reaches 100%, quantitative selectivity toward N_2 was observed, thus CO_2 production occurred at a 1:1 ratio with NO and CO consumption. We can derive site-specific overall reactions for NO reduction by CO in wet environments, where in the case of Rh clusters $2NO + 2CO \rightarrow N_2 + 2CO_2$ occurs, whereas for atomically dispersed Rh $2NO + 3H_2O + 5CO \rightarrow 2NH_3 + 5CO_2$ occurs.

For the 0.05 and 0.1 Rh wt % cases, there was an excess of CO_2 formed after complete NO conversion that was not accounted for by the reactions proposed above. A plausible source of CO_2 production is through the water−gas shift reaction ($H_2O + CO \rightarrow H_2 + CO_2$, WGS) occurring over atomically dispersed Rh species. To test this hypothesis, light-off curves were obtained with 2% H_2O and at CO levels equivalent to the balance of CO after complete NO consumption, Figure S5. For the 0.05 Rh wt % catalyst, CO_2 started forming at ∼275 °C and gradually increased to ∼1000 ppm by the end of the run, Figure S5. This is consistent with the excess CO_2 formed over atomically dispersed Rh samples at temperatures where NO conversion was complete. This behavior is also consistent with previous work showing that

https://dx.doi.org/10.1021/acscatal.0c01249
ACS Catal. 2020, 10, 5217−5222

various atomically dispersed metal catalysts, and specifically Rh, are highly active for WGS.[35,48,56−58] The 5 wt % Rh catalyst did not light off WGS until >300 °C, accounting for the lack of excess CO_2 on catalysts consisting primarily of Rh clusters.

Including WGS over atomically dispersed Rh closes the mass balance for all products over the tested temperature range. However, in the cases of 0.1, 0.2, and 2 wt % Rh, there was an apparent spike of excess N_2 produced during the initial NO conversion light off, Figure S4a. The amount of N_2 produced was calculated by mass balance assuming N_2, NO, N_2O, and NH_3 are the only N-containing species. It was hypothesized that NH_3 formed during initial light off adsorbs to acidic sites inherent to the Al_2O_3 support, so there was a delay in formed NH_3 exiting the reactor while NO was being consumed until all acidic sites were titrated.[59,60] To test this hypothesis, a steady-state experiment was performed where a feed consisting of 1000 ppm of NO, 5000 ppm of CO, and 2% water was introduced to the 0.1 Rh wt % catalyst for extended time at 185, 195, 205, and 215 °C (Figure S6). The steady-state amount of NH_3 reached 2.5:1 stochiometric balance with CO_2 at all temperatures in agreement with the proposed reaction, demonstrating that NH_3 adsorption to the catalyst surface likely was occurring during initial light off.

We also explored whether the structure−function relationship developed for Rh/Al_2O_3 would apply to CeO_2 supports (US-Nano stock #US3037, 70 m^2/g), which are also of relevance to catalytic converters (Figure S7).[49] At 0.2 wt % Rh on CeO_2, where CO FTIR suggested Rh is predominantly atomically dispersed, the catalyst was 100% selective toward NH_3 during the wet light-off experiment. The reaction lights off at a lower temperature on atomically dispersed Rh on CeO_2 as compared with Al_2O_3 by ∼25 °C, suggesting inherently higher reactivity on the reducible support. At 2 wt % Rh loading, where the presence of Rh clusters is evidenced in the CO FTIR, selectivity toward N_2 increased suggesting Rh clusters are selective for N_2 on either support.

The strong correlation between the fraction of exposed sites existing as atomically dispersed Rh species in initial characterization and the amount of NH_3 produced during reactivity measurements with co-fed H_2O provide strong evidence that atomically dispersed Rh species on Al_2O_3 and CeO_2 are active at low temperature for NH_3 formation, suggesting this is a critical active site in TWC. Recent reports of analysis of atomically dispersed Rh and Pt species in TWCs did not identify this active site relationship either due to focus on oxidation reactions, the lack of inclusion of H_2O in the feed, or focus on trends in conversion and stability.[28,61−63] Within a ∼50 °C window, we found that NH_3 formation and WGS over atomically dispersed Rh occurred simultaneously with N_2 formation over Rh clusters, making it challenging to understand the catalytic behavior of materials containing a mix of active site types, as portrayed in Figure 3.

The present work demonstrates that even for a simple feed containing only NO, CO, and H_2O, dramatic differences in rate and selectivity on active sites of differing Rh nuclearity are observed. Additional species present in combustion exhaust, including oxygen and hydrocarbons, may also alter selectivity not only by introducing competing reaction pathways or inhibiting kinetically relevant steps in NO reduction, but also potentially by altering the distribution of active site nuclearity. Thus, while it is not reasonable to hypothesize a complete mechanistic pathway for NH_3 formation over atomically dispersed species, it is likely that the mechanism is distinct from NO reduction pathways on extended Rh surfaces, which proceed through NO dissociation. It is hypothesized that NH_3 formation on atomically dispersed Rh shares mechanistic steps with the water gas shift reaction, which occurs at lower temperatures on atomically dispersed Rh as compared to Rh clusters and is promoted by reducible supports.[64] Further, it is expected that Rh structure and coordination to the support may be quite dynamic under the complex feed conditions of TWC, a consideration that will be critical for future mechanistic analyses.

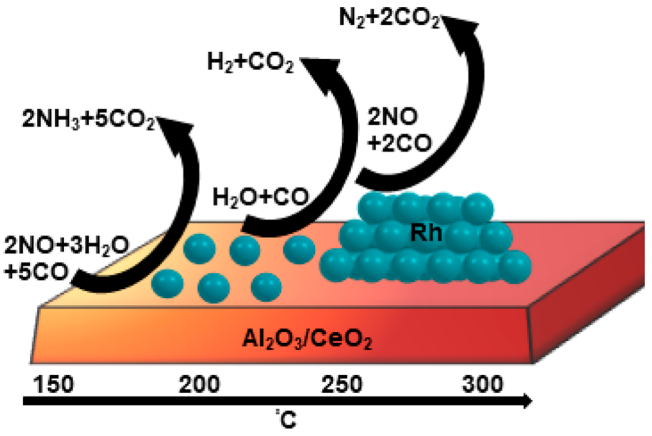

Figure 3. Depiction of product formation during NO reduction over different Rh structures on oxide supports at increasing temperature between 150 to 300 °C. $2NO + 3H_2O + 5CO \rightarrow 2NH_3 + 5CO_2$ occurs over atomically dispersed Rh at ∼180 °C, $H_2O + CO \rightarrow H_2 + CO_2$ (WGS) occurs over atomically dispersed Rh at ∼250 °C, and $2NO + 2CO \rightarrow N_2 + 2CO_2$ occurs over Rh clusters at ∼250 °C.

In conclusion, we provide evidence that atomically dispersed Rh species selectively produce NH_3 at low temperature in the reduction of NO by CO when H_2O is present. These conclusions indicate that reformulating the TWC in catalytic converters to prevent the formation of atomically dispersed Rh could reduce NH_3 emissions from gasoline burning automobiles. This study also clearly identifies the important role of minimizing the distribution of active site types in catalytic materials to facilitate structure−function relationship elucidation.

■ ASSOCIATED CONTENT

Supporting Information

The Supporting Information is available free of charge at https://pubs.acs.org/doi/10.1021/acscatal.0c01249.

Catalyst synthesis, characterization procedure, light-off experimental procedure, and supporting figures (PDF)

■ AUTHOR INFORMATION

Corresponding Author

Phillip Christopher − *Department of Chemical Engineering, University of California, Santa Barbara 93117, United States;* orcid.org/0000-0002-4898-5510; Email: pchristopher@ucsb.edu

Authors

Chithra Asokan − *Department of Chemical Engineering, University of California, Santa Barbara 93117, United States*

Yang Yang − *Department of Chemical Engineering, University of California, Santa Barbara 93117, United States*

https://dx.doi.org/10.1021/acscatal.0c01249
ACS Catal. 2020, 10, 5217−5222

Alan Dang − *Department of Chemical Engineering, University of California, Santa Barbara 93117, United States*
Andrew "Bean" Getsoian − *Research and Advanced Engineering, Ford Motor Company, Dearborn 48124, United States*

Complete contact information is available at: https://pubs.acs.org/10.1021/acscatal.0c01249

Notes

The authors declare no competing financial interest.

■ ACKNOWLEDGMENTS

This work was supported by Science Foundation (NSF) GOALI Grant CBET-1804128 and Mellichamp Initiative for Sustainability at the University of California, Santa Barbara.

■ REFERENCES

(1) Behera, S. N.; Sharma, M. Science of the Total Environment Investigating the Potential Role of Ammonia in Ion Chemistry of Fine Particulate Matter Formation for an Urban Environment. *Sci. Total Environ.* **2010**, *408* (17), 3569−3575.
(2) Gong, L.; Lewicki, R.; Griffin, R. J.; Tittel, F. K.; Lonsdale, C. R.; Stevens, R. G.; Pierce, J. R.; Malloy, Q. G. J.; Travis, S. A.; Bobmanuel, L. M.; Lefer, B. L.; Flynn, J. H. Role of Atmospheric Ammonia in Particulate Matter Formation in Houston during Summertime. *Atmos. Environ.* **2013**, *77*, 893−900.
(3) Bergstrom, A.; Jansson, M. Atmospheric Nitrogen Deposition Has Caused Nitrogen Enrichment and Eutrophication of Lakes in the Northern Hemisphere. *Glob. Chang. Biol.* **2006**, *12* (4), 635−643.
(4) Fangmeier, A.; Hadwiger-Fangmeier, A.; Van der Eerden, L.; Jager, H.-J. Effects of Atmospheric Ammonia on Vegetation—a Review. *Environ. Pollut.* **1994**, *86* (1), 43−82.
(5) Heeb, N. V.; Forss, A.-M.; Brühlmann, S.; Lüscher, R.; Saxer, C. J.; Hug, P. Three-Way Catalyst-Induced Formation of Ammonia—Velocity-and Acceleration-Dependent Emission Factors. *Atmos. Environ.* **2006**, *40* (31), 5986−5997.
(6) Prikhodko, V. Y.; Parks, J. E.; Pihl, J. A.; Toops, T. J. Ammonia Generation and Utilization in a Passive SCR (TWC+SCR) System on Lean Gasoline Engine. *SAE Int. J. Engines* **2016**, *9* (2), 1289−1295.
(7) Macleod, N.; Isaac, J.; Lambert, R. M. A Comparison of Sodium-Modified Rh/γ-Al2O3 and Pd/γ-Al2O3 Catalysts Operated under Simulated TWC Conditions. *Appl. Catal., B* **2001**, *33* (4), 335−343.
(8) Wang, C.; Tan, J.; Harle, G.; Gong, H.; Xia, W.; Zheng, T.; Yang, D.; Ge, Y.; Zhao, Y. Ammonia Formation over Pd/Rh Three-Way Catalysts during Lean-to-Rich Fluctuations: The Effect of the Catalyst Aging, Exhaust Temperature, Lambda, and Duration in Rich Conditions. *Environ. Sci. Technol.* **2019**, *53* (21), 12621−12628.
(9) Shelef, M.; Graham, G. W. Why Rhodium in Automotive Three-Way Catalysts? *Catal. Rev.: Sci. Eng.* **1994**, *36* (3), 433−457.
(10) Digiulio, C. D.; Pihl, J. A.; Parks, J. E., II; Amiridis, M. D.; Toops, T. J. Passive-Ammonia Selective Catalytic Reduction (SCR): Understanding NH 3 Formation over Close-Coupled Three Way Catalysts (TWC). *Catal. Today* **2014**, *231* (X), 33−45.
(11) Hibbitts, D. D.; Jiménez, R.; Yoshimura, M.; Weiss, B.; Iglesia, E. Catalytic NO Activation and NO−H2 Reaction Pathways. *J. Catal.* **2014**, *319*, 95−109.
(12) Dümpelmann, R.; Cant, N. W.; Trimm, D. L. The Positive Effect of Hydrogen on the Reaction of Nitric Oxide with Carbon Monoxide over Platinum and Rhodium Catalysts. *Catal. Lett.* **1995**, *32* (3−4), 357−369.
(13) Oh, S. H.; Triplett, T. Reaction Pathways and Mechanism for Ammonia Formation and Removal over Palladium-Based Three-Way Catalysts: Multiple Roles of CO. *Catal. Today* **2014**, *231*, 22−32.
(14) Oh, S. H.; Fisher, G. B.; Carpenter, J. E.; Goodman, D. W. Comparative Kinetic Studies of CO-O2 and CO-NO Reactions over Single Crystal and Supported Rhodium Catalysts. *J. Catal.* **1986**, *100* (2), 360−376.
(15) Zhdanov, V. P.; Kasemo, B. Mechanism and Kinetics of the NO— CO Reaction on Rh. *Surf. Sci. Rep.* **1997**, *29* (2), 31−90.
(16) Hecker, W. C.; Bell, A. T. Reduction of NO by CO over Silica-Supported Rhodium: Infrared and Kinetic Studies. *J. Catal.* **1983**, *84* (1), 200−215.
(17) Araya, P.; Gracia, F.; Cortés, J.; Wolf, E. E. FTIR Study of the Reduction Reaction of NO by CO over Rh/SiO2 Catalysts with Different Crystallite Size. *Appl. Catal., B* **2002**, *38* (2), 77−90.
(18) Hendriksen, D. E.; Meyer, C. D.; Eisenberg, R. Nature of the Active Catalyst in the Rhodium Complex Catalyzed Reduction of Nitric Oxide by Carbon Monoxide. *Inorg. Chem.* **1977**, *16* (4), 970−972.
(19) Goldsmith, B. R.; Sanderson, E. D.; Ouyang, R.; Li, W. X. CO- and NO-Induced Disintegration and Redispersion of Three-Way Catalysts Rhodium, Palladium, and Platinum: An Ab Initio Thermodynamics Study. *J. Phys. Chem. C* **2014**, *118* (18), 9588−9597.
(20) Guzman, J.; Gates, B. C. Supported Molecular Catalysts: Metal Complexes and Clusters on Oxides and Zeolites. *Dalt. Trans.* **2003**, *17*, 3303−3318.
(21) Getsoian, A.; Theis, J. R.; Paxton, W. A.; Lance, M. J.; Lambert, C. K. Remarkable Improvement in Low Temperature Performance of Model Three-Way Catalysts through Solution Atomic Layer Deposition. *Nat. Catal.* **2019**, *2* (7), 614−622.
(22) Tan, L.; Huang, L.; Liu, Y.; Wang, Q. Detailed Mechanism of the NO + CO Reaction on Rh(1 0 0) and Rh(1 1 1): A First-Principles Study. *Appl. Surf. Sci.* **2018**, *444*, 276−286.
(23) Deushi, F.; Ishikawa, A.; Nakai, H. Density Functional Theory Analysis of Elementary Reactions in NOxReduction on Rh Surfaces and Rh Clusters. *J. Phys. Chem. C* **2017**, *121* (28), 15272−15281.
(24) Chafik, T.; Kondarides, D. I.; Verykios, X. E. Catalytic Reduction of NO by CO over Rhodium Catalysts: 1. Adsorption and Displacement Characteristics Investigated by In Situ FTIR and Transient-MS Techniques. *J. J. Catal.* **2000**, *190* (2), 446−459.
(25) McCabe, R. W.; Wong, C. Steady-State Kinetics of the CON2O Reaction over an Alumina-Supported Rhodium Catalyst. *J. Catal.* **1990**, *121* (2), 422−431.
(26) Almusaiteer, K. A.; Chuang, S. S. C. Infrared Characterization of Rh Surface States and Their Adsorbates during the NO-CO Reaction. *J. Phys. Chem. B* **2000**, *104* (10), 2265−2272.
(27) Granger, P.; Dhainaut, F.; Pietrzik, S.; Malfoy, P.; Mamede, A. S.; Leclercq, L.; Leclercq, G. An Overview: Comparative Kinetic Behaviour of Pt, Rh and Pd in the NO+CO and NO+H2 Reactions. *Top. Catal.* **2006**, *39* (1−2), 65−76.
(28) Vityuk, A. D.; Ma, S.; Alexeev, O. S.; Amiridis, M. D. NO Reduction with CO over HY Zeolite-Supported Rhodium Dicarbonyl Complexes: Giving Insight into the Structure Sensitivity. *React. Chem. Eng.* **2019**, *4* (2), 418−426.
(29) Matsubu, J. C.; Yang, V. N.; Christopher, P. Isolated Metal Active Site Concentration and Stability Control Catalytic CO2 Reduction Selectivity. *J. Am. Chem. Soc.* **2015**, *137* (8), 3076−3084.
(30) Qi, J.; Christopher, P. Atomically Dispersed Rh Active Sites on Oxide Supports with Controlled Acidity for Gas-Phase Halide-Free Methanol Carbonylation to Acetic Acid. *Ind. Eng. Chem. Res.* **2019**, *58* (28), 12632−12641.
(31) Shan, J.; Li, M.; Allard, L. F.; Lee, S.; Flytzani-Stephanopoulos, M. Mild Oxidation of Methane to Methanol or Acetic Acid on Supported Isolated Rhodium Catalysts. *Nature* **2017**, *551* (7682), 605−608.
(32) Serna, P.; Gates, B. C. Zeolite-Supported Rhodium Complexes and Clusters: Switching Catalytic Selectivity by Controlling Structures of Essentially Molecular Species. *J. Am. Chem. Soc.* **2011**, *133* (13), 4714−4717.
(33) Santos, P. S.; Santos, H. S.; Toledo, S. P. Standard Transition Aluminas. Electron Microscopy Studies. *Mater. Res.* **2000**, *3* (4), 104−114.
(34) Asokan, C.; Derita, L.; Christopher, P. Using Probe Molecule FTIR Spectroscopy to Identify and Characterize Pt - Group Metal

Based Single Atom Catalysts. *Chin. J. Catal.* **2017**, *38* (9), 1473−1480.
(35) Tang, Y.; Asokan, C.; Xu, M.; Graham, G. W.; Pan, X.; Christopher, P.; Li, J.; Sautet, P. Rh Single Atoms on TiO2 Dynamically Respond to Reaction Conditions by Adapting Their Site. *Nat. Commun.* **2019**, *10* (1), 4488.
(36) Hyde, E. A.; Rudham, R.; Rochester, C. H. Infrared Study of the Interactions between NO and CO on Rh/Al2O3 Catalysts. *J. Chem. Soc., Faraday Trans. 1* **1984**, *80* (3), 531−541.
(37) Granger, P.; Delannoy, L.; Lecomte, J. J.; Dathy, C.; Praliaud, H.; Leclercq, L.; Leclercq, G. Kinetics of the CO + NO Reaction over Bimetallic Platinum-Rhodium on Alumina: Effect of Ceria Incorporation into Noble Metals. *J. Catal.* **2002**, *207* (2), 202−212.
(38) Lamberti, C.; Zecchina, A.; Groppo, E.; Bordiga, S. Probing the Surfaces of Heterogeneous Catalysts by in Situ IR Spectroscopy. *Chem. Soc. Rev.* **2010**, *39* (12), 4951.
(39) Asokan, C.; Thang, H. V.; Pacchioni, G.; Christopher, P. Reductant Composition Influences the Coordination of Atomically Dispersed Rh on Anatase TiO2. *Catal. Sci. Technol.* **2020**, *10* (6), 1597−1601.
(40) Yang, C.; Garl, C. W. Infrared Studies of Carbon Monoxide Chemisorbed on Rhodium. *J. Phys. Chem.* **1957**, *61* (11), 1504−1512.
(41) Yates, J. T.; Duncan, T. M.; Worley, S. D.; Vaughan, R. W. Infrared Spectra of Chemisorbed CO on Rh. *J. Chem. Phys.* **1979**, *70* (3), 1219.
(42) Goellner, J. F.; Gates, B. C.; Vayssilov, G. N.; Rösch, N. Structure and Bonding of a Site-Isolated Transition Metal Complex: Rhodium Dicarbonyl in Highly Dealuminated Zeolite Y. *J. Am. Chem. Soc.* **2000**, *122* (33), 8056−8066.
(43) Duncan, T. M.; Yates, J. T.; Vaughan, R. W. A 13C NMR Study of the Adsorbed States of CO on Rh Dispersed on Al2O3. *J. Chem. Phys.* **1980**, *73* (2), 975−985.
(44) Brown, T. L.; Darensbourg, D. J. Intensities of CO Stretching Modes in the Infrared Spectra of Adsorbed CO and Metal Carbonyls. *Inorg. Chem.* **1967**, *6* (5), 971−977.
(45) Van't Blik, H. F. J.; Van Zon, J.; Huizinga, T.; Vis, J. C.; Koningsberger, D. C.; Prins, R. Structure of Rhodium in an Ultradispersed Rhodium/Alumina Catalyst as Studied by EXAFS and Other Techniques. *J. Am. Chem. Soc.* **1985**, *107* (11), 3139−3147.
(46) Robbins, J. L. Rhodium Dicarbonyl Sites on Alumina Surfaces. 1. Preparation and Characterization of a Model System. *J. Phys. Chem.* **1986**, *90* (15), 3381−3386.
(47) Buchanan, D. A.; Hernandez, M. E.; Solymosi, F.; White, J. M. CO-Induced Structural Changes of Rh on TiO2 Support. *J. Catal.* **1990**, *125* (2), 456−466.
(48) Guan, H.; Lin, J.; Qiao, B.; Miao, S.; Wang, A.; Wang, X.; Zhang, T. Enhanced Performance of Rh 1/TiO 2 Catalyst Without Methanation in Water-Gas Shift Reaction. *AIChE J.* **2017**, *63* (6), 2081−2088.
(49) Resasco, J.; DeRita, L.; Dai, S.; Chada, J. P.; Xu, M.; Yan, X.; Finzel, J.; Hanukovich, S.; Hoffman, A. S.; Graham, G. W.; Bare, S. R.; Pan, X.; Christopher, P. Uniformity Is Key in Defining Structure−Function Relationships for Atomically Dispersed Metal Catalysts: The Case of Pt/CeO2. *J. Am. Chem. Soc.* **2020**, *142* (1), 169−184.
(50) DeRita, L.; Resasco, J.; Dai, S.; Boubnov, A.; Thang, H. V.; Hoffman, A. S.; Ro, I.; Graham, G. W.; Bare, S. R.; Pacchioni, G.; Pan, X.; Christopher, P. Structural Evolution of Atomically Dispersed Pt Catalysts Dictates Reactivity. *Nat. Mater.* **2019**, *18* (7), 746−751.
(51) Rice, C. A.; Worley, S. D.; Curtis, C. W.; Guin, J. A.; Tarrer, A. R. The Oxidation State of Dispersed Rh on AI2O3. *J. Chem. Phys.* **1981**, *74* (11), 6487−6497.
(52) Yates, J. T.; Duncan, T. M.; Worley, S. D.; Vaughan, R. W. Infrared Spectra of Chemisorbed CO on Rh. *J. Chem. Phys.* **1979**, *70* (3), 1219.
(53) Cavanagh, R. R.; Yates, J. T., Jr. Site Distribution Studies of Rh Supported on Al2O3—An Infrared Study of Chemisorbed CO. *J. Chem. Phys.* **1981**, *74* (7), 4150.
(54) Getsoian, A. B.; Theis, J. R.; Lambert, C. K. Sensitivity of Three-Way Catalyst Light-Off Temperature to Air-Fuel Ratio. *Emiss. Control Sci. Technol.* **2018**, *4* (3), 136−142.
(55) Coller, D. H.; Vicente, B. C.; Scott, S. L. Rapid Extraction of Quantitative Kinetic Information from Variable-Temperature Reaction Profiles. *Chem. Eng. J.* **2016**, *303*, 182−193.
(56) Flytzani-stephanopoulos, M. Gold Atoms Stabilized on Various Supports Catalyze the Water A Gas Shift Reaction. *Acc. Chem. Res.* **2014**, *47* (3), 783−792.
(57) Lin, J.; Wang, A.; Qiao, B.; Liu, X.; Yang, X.; Wang, X.; Liang, J.; Li, J.; Liu, J.; Zhang, T. Remarkable Performance of Ir1/FeOx Single-Atom Catalyst in Water Gas Shift Reaction. *J. Am. Chem. Soc.* **2013**, *135* (41), 15314−15317.
(58) Ghosh, T. K.; Nair, N. N. Rh 1/g -Al 2 O 3 Single-Atom Catalysis of O 2 Activation and CO Oxidation: Mechanism, Effects of Hydration, Oxidation State, and Cluster Size. *ChemCatChem* **2013**, *5* (7), 1811−1821.
(59) Tamura, M.; Shimizu, K.; Satsuma, A. Applied Catalysis A: General Comprehensive IR Study on Acid/Base Properties of Metal Oxides. *Appl. Catal., A* **2012**, *433*, 135−145.
(60) Busca, G. The Surface Acidity of Solid Oxides and Its Characterization by IR Spectroscopic Methods. An Attempt at Systematization. *Phys. Chem. Chem. Phys.* **1999**, *1* (5), 723−736.
(61) Jeong, H.; Kwon, O.; Kim, B.; Bae, J.; Shin, S.; Kim, H.; Kim, J.; Lee, H. Highly Durable Metal Ensemble Catalysts with Full Dispersion for Automotive Applications beyond Single-Atom Catalysts. *Nat. Catal.* **2020**, *3*, 368−375.
(62) Jeong, H.; Lee, G.; Kim, B.; Bae, J.; Han, J. W.; Lee, H. Fully Dispersed Rh Ensemble Catalyst To Enhance Low-Temperature Activity. *J. Am. Chem. Soc.* **2018**, *140* (30), 9558−9565.
(63) Fernandez, E.; Liu, L.; Boronat, M.; Arenal, R.; Concepcion, P.; Corma, A. Low-Temperature Catalytic NO Reduction with CO by Subnanometric Pt Clusters. *ACS Catal.* **2019**, *9* (12), 11530−11541.
(64) Li, T.; Chen, F.; Lang, R.; Wang, H.; Su, Y.; Qiao, B.; Wang, A.; Zhang, T. Styrene Hydroformylation with In Situ Hydrogen: Regioselectivity Control by Coupling with the Low-Temperature Water − Gas Shift Reaction. *Angew. Chem.* **2020**, *59*, 1−6.

https://dx.doi.org/10.1021/acscatal.0c01249
ACS Catal. 2020, 10, 5217−5222